

1 **Climate-induced mortality of Siberian pine and fir in the Lake Baikal Watershed,**  
2 **Siberia**

3  
4 **Viacheslav I. Kharuk<sup>1,2\*</sup>, Sergey T. Im<sup>1,2,3</sup>, Ilya A. Petrov<sup>1</sup>, Alexei S. Golyukov<sup>1,2</sup>, Kenneth J.**  
5 **Ranson<sup>4</sup> and Mikhail N. Yagunov<sup>5</sup>**

6  
7 <sup>1</sup>*Sukachev Institute of Forest, 660036, Krasnoyarsk, Russia,*

8 <sup>2</sup>*Siberian Federal University, 660041, Krasnoyarsk, Russia,*

9 <sup>3</sup>*Siberian State Aerospace University, 660014, Krasnoyarsk, Russia,*

10 <sup>4</sup>*NASA's Goddard Space Flight Center, Greenbelt, MD 20771, USA.*

11 <sup>5</sup>*Russian Center of Forest Protection, 660036, Krasnoyarsk, Russia*

12

13 **Running title: Conifer mortality within the Lake Baikal watershed**

14

15 \*Correspondence: Viacheslav Kharuk,

16 Sukachev Institute of Forest, Academgorodok 50/28, 660036 Krasnoyarsk, Russia

17 Email: kharuk@ksc.krasn.ru, tel: +7-391-243-88-25

18 **ABSTRACT**

19 Siberian pine (*Pinus sibirica*) and fir (*Abies sibirica*) (so called “dark needle conifers”, DNC) showed  
20 decreased radial growth increment within the Lake Baikal watershed since the 1980s with increasing  
21 mortality recorded since the year 2000. Tree ring width was strongly correlated with vapor pressure  
22 deficit, aridity and root zone moisture. Water stress from droughts made trees more susceptible to  
23 insect attacks causing mortality in about 10% of DNC stands within the Lake Baikal watershed.  
24 Within Siberia DNC mortality increased in the southern part of the DNC range. Biogeographically,  
25 tree mortality was located within the DNC – forest-steppes transition. Tree mortality was significantly  
26 correlated with drought and soil moisture anomalies. Within the interior of the DNC range mortality  
27 occurred within relief features with high water stress risk (i.e., steep convex south facing slopes with  
28 shallow well-drained soils). In general, DNC mortality in Siberia was induced by increased aridity and  
29 severe drought (inciting factors) in synergy with biotic attacks (contributing factor). In future climate  
30 scenarios with predicted increase in aridity DNC could be eliminated from the southern part of its  
31 current range and will be replaced by drought-resistant conifers and broadleaf species (e.g., *Larix*  
32 *sibirica*, *Pinus silvestris*, and *Betula pubescence*).

33  
34 Keywords: water stress, conifer mortality, Lake Baikal Region, drought, aridity increase, forest health

## 35 1. Introduction

36 Conifer decline (i.e., tree vigor decrease) and mortality was reported for a number of sites  
37 within the boreal zone (Lloyd and Bunn, 2007; Aitken et al., 2008; Millar and Stephenson, 2015).  
38 *Pinus ponderosa* decline has occurred in the North American forests (Logan et al., 2003; Fettig et al.,  
39 2013). Dieback or degradation of thousands of ha of spruce forests has been observed in Ukraine and  
40 in Baltic and European countries (Allen et al., 2009; Yousefpour et al., 2010; Martínez-Vilalta et al.,  
41 2012; Kharuk et al., 2015a). Large amounts of tree mortality were also reported in *Picea abies* stands  
42 in Belarus (Sarnatskii, 2012; Kharuk et al., 2016). Large-scale spruce mortality decline has been  
43 observed in the European part of Russia (Chuprov, 2008; Zamolodchikov, 2011). In the Russian Far  
44 East *Picea ajansis* and *Abies nephrolepis* die-off was documented (Man'ko et al., 1998). Siberian pine  
45 and fir stands mortality have been observed in the region of Lake Baikal and the southern Siberian  
46 Mountains (Kharuk et al., 2013a). Conifer mortality was attributed to bacterial diseases (Raffa et al.,  
47 2008; Review of forest health..., 2010), root fungi and insects attacks (Logan et al., 2003; Pavlov et al.,  
48 2008; Chuprov, 2008; Kolb et al., 2016), and drought increase (Millar and Stephenson, 2015; Kharuk  
49 et al., 2013a,b; Kharuk et al., 2015a).

50 In recent decades, Lake Baikal watershed forests experienced decline and mortality. These  
51 forests are composed of Siberian pine (*Pinus sibirica*) and fir (*Abies sibirica*) with a mixture of spruce  
52 (*Picea obovata*) [so called “dark needle conifer” (DNC)] species. The main causes of DNC mortality  
53 were considered to be biotic and anthropogenic impacts (Review of forest health..., 2010). These local  
54 watershed forests are a primary supplier of water for Lake Baikal, which is the largest (20% of the  
55 world's fresh water), deepest (1,642 m depth), and oldest (25 million years) lake in the world.

56 The main goal of this paper is to provide an analysis of causes of DNC mortality within (1)  
57 Lake Baikal watersheds and (2) within the DNC species range in Siberia. The hypothesis tested is  
58 DNC mortality was caused by increased aridity and severe drought (inciting factors) in synergy with  
59 bark and wood boring insects and fungi attacks (contributing factors).

## 60 2. Methods

61 The studies were based upon on-ground observations, dendrochronology, environmental  
62 variables (air temperature, precipitation, root zone wetness, vapor pressure deficit, drought index  
63 SPEI), remote sensing and GIS-technologies.

## 64 2.1. Study area

65 The studied stands are located in the Lake Baikal watershed (Khamar-Daban Ridge, Fig. 1). The  
 66 ridge is 60 km × 350 km in dimension with maximum height of about 2,370 m. Pine and fir stands are  
 67 dominant at elevations up to 1,500–1,600 m. The treeline is formed by Siberian pine. The subalpine  
 68 belt (up to 1,700 m) included meadows, shrubs and sparse trees (*Pinus sibirica* and *Abies sibirica*).  
 69 Tundra communities are typical at higher elevations (i.e. >1,700 m).

## 70 2.2. Climate

71 Environmental variables considered for this study included air temperature, precipitation,  
 72 drought index SPEI (Standardized Precipitation-Evaporation Index) and root zone wetness. SPEI is a  
 73 measure of drought intensity and duration (Vicente-Serrano et al., 2010), and is defined as the  
 74 difference between precipitation and potential evapotranspiration:

75

$$76 D_i = P_i - PET_i ,$$

77

78 where  $i$  is the time period.

79  $PET$  (mm) is calculated as:

80

$$81 PET = 16 \times K \times (10 \times T \times I^1)^m ,$$

82

83 where  $T$  is the monthly mean temperature in °C;  $I$  is a heat index,  $m$  is a coefficient depending on  $I$ ,  
 84 and  $K$  is a correction coefficient. SPEI data (0.5° × 0.5° spatial resolution) was obtained from  
 85 <http://sac.csic.es/spei>.

86 Mean air temperatures within the study area were 14–18 °C in July and -11...-25 °C in  
 87 December-February. The mean annual air temperature in the mountains and on the shore of Lake  
 88 Baikal are -3.4 °C and about 0° C, respectively. Maximum precipitation occurred in late July-August,  
 89 and the minimum in spring and autumn. Maximum aridity was observed in June-July (Appendix Fig.  
 90 A1d). Summer air temperature showed a positive trend in 1980–2002 (Appendix Fig. A1a). Drought  
 91 increased since the 1980s (Appendix Fig. A1c). No trends in precipitation were found for the studied  
 92 time period. Climate variables were obtained from “Kabansk” (52°05’N, 106°65’E; 466 m a.s.l.) and  
 93 “Khamar-Daban” (51°53’N, 103°59’E; 1,442 m a.s.l.) weather stations located on the shore of Lake  
 94 Baikal and in the nearby mountains, respectively.

### 95 2.3. Field studies

96 Field studies were conducted during July 2015 within an area known for major forest mortality  
 97 (Fig. 1). Temporary test sites (TS,  $N = 23$ ) were established along an elevational transect across the  
 98 ridge. The transect began at the northern boundary of the declining stands and ended on the southern  
 99 boundary. This transect included areas with high levels of tree mortality ( $>25\%$  of trees), as well as  
 100 stands without symptoms of decline. The following data were collected within each TS: tree inventory,  
 101 soil, ground cover, and a description of topography (i.e., elevation, azimuth, slope steepness, terrain  
 102 curvature (convex/concave)). A tree inventory (i.e., species composition, tree height, diameter at  
 103 breast height (dbh), tree vigor) was conducted within circular plots of radius = 9.8 m. These data were  
 104 also used for satellite data interpretation. Samples for dendrochronological analysis were taken by  
 105 increment borer or chainsaw at breast height (1.3 m). Sampled trees were randomly chosen around the  
 106 TS centerpoint within a 0.5 ha area and a  $\pm 10$  m range of elevation.

107 Study stands were composed of Siberian pine and Siberian fir trees. Mean tree heights and  
 108 (dbh) were 17 m (43 cm) and 13 m (18 cm) for Siberian pine and fir, respectively. Mean age was 130  
 109 years for pine and 90 years for fir. Shrubs were represented by *Juniperus sibirica*, *Duschekia fruticosa*,  
 110 *Spiraea salicifolia*. Ground cover consisted of *Bergenia crassifolia*, *Vaccinium myrtillus*, *Cárex sp.*,  
 111 and different species of mosses and lichens. Soils were well-drained sandy brown-mountain. Horizons  
 112  $A_0$  and  $C_0$  (bedrock level) were at 1–5 and 15–25 cm, respectively.

113 Within the DNC range in Siberia, Russian State Forest Service collected forest pathology data  
 114 from 2008 to 2015. The dataset included tree's vigor status and causes of mortality (fires, insect  
 115 attacks, climate impact, windfall, diseases, etc.). In this analysis we used data for insect attacks,  
 116 climate impact, and diseases (total number of test plots was  $N = 9681$ , including 6046 of "insect  
 117 attacks", 268 of "climate impact", and 3367 of "diseases"). That dataset was used in geospatial  
 118 analysis of the relationships between tree mortality and drought index and root zone wetness.

### 119 2.4. Remote sensing data and GIS analysis

120 DNC mortality was also analyzed based on data from multiple satellites. 1) Moderate resolution  
 121 (30 m) Landsat data consisting of Landsat 8/OLI acquired 25.06.2015 and 18.06.2015; Landsat 5/TM  
 122 acquired 30.09.1989 and 15.10.1992; and Landsat 4/MSS acquired 29.09.1989. (data source was  
 123 <http://glovis.usgs.gov>), 2) High resolution imagery (0.41–0.5 m) from Worldview and GeoEye  
 124 satellites was acquired 18.08.2010, 17.09.2010, 11.09.2010 and provided through NASA's NGA  
 125 Commercial Archive Data ([cad4nasa.gsfc.nasa.gov](http://cad4nasa.gsfc.nasa.gov)). 3) Topographic information was provided by  
 126 NASA's Shuttle Radar Topography Mission (SRTM) digital elevation model (DEM) at 30 m

127 resolution and available at (<http://earthexplorer.usgs.gov>). Soil water content/anomalies were analyzed  
128 based on NASA GRACE from ([podaac.jpl.nasa.gov](http://podaac.jpl.nasa.gov)) and SMAP satellite data acquired from NASA's  
129 Snow and Ice Data Center (<https://nsidc.org/data/smap/smap-data.html>). We used the SRTM DEM for  
130 analysis of the relationship between DNC mortality with relief features (elevation, slope steepness,  
131 curvature, and exposure). Exposure or slope aspect was analyzed for eight directions (north ( $0^\circ$ ),  
132 northeast ( $45^\circ$ ), east ( $90^\circ$ ), etc.); slope steepness was analyzed with one-degree intervals. Curvature  
133 was presented in relative units (negative values for concave and positive for convex surface).

#### 134 2.5. *Stand mortality detection*

135 Declined stands were detected using Landsat data and maximum likelihood classification with a  
136 threshold procedure ( $p$ -value = 0.05). First a mask of dark-needle stands was generated for the period  
137 prior to tree mortality (1989). For this purpose 10 training areas (TA) of DNC stands were generated  
138 with average size of  $699 \pm 117$  pixels). Then, a mask of DNC was generated. Dead stands were detected  
139 on the Landsat (2015) scenes based on 30 TA (approx. 600 pixels each). TA were generated based on  
140 ground-truth data and high-resolution WorldView and GeoEye imagery. Spatial resolution of the  
141 scenes provided identification of individual trees. Furthermore, the following stand categories were  
142 identified: healthy and slightly damaged stands (mortality < 25%), moderately damaged stands (25–  
143 50%), heavily damaged stands (50–75%), and areas of tree mortality (> 75%). However, upon further  
144 analysis the first two categories were merged because of their low separability. Classification  
145 accuracies were estimated using KHAT ( $\kappa$ )-statistics (Congalton, 1991).

#### 146 2.6. *Data processing*

147 Remote sensing data were processed using Erdas Imagine software  
148 (<http://geospatial.intergraph.com>). GIS-analysis was carried out using ESRI ArcGIS software package  
149 (<http://www.esri.com>). Statistical analysis was realized using Microsoft Excel and Statsoft Statistica  
150 software (<http://www.statsoft.ru>). The C-correction algorithm for topographic correction of Riano et  
151 al., (2003) was applied to the Landsat scenes using the SRTM DEM.

## 152 2.7. Drought and soil moisture assessment

### 153 2.7.1. Soil Moisture Active Passive (SMAP) product

154 The Soil Moisture Active Passive (SMAP) mission was launched in January 2015 with two  
 155 sensors to provide information on surface soil moisture (<http://smap.jpl.nasa.gov>). The first sensor  
 156 (passive) measures land surface microwave emission at 1.41 GHz and provides profile data with 36 km  
 157 spatial resolution. The second one was an active sensor, which measured radar backscatter (at 1.26  
 158 GHz and 1.29 GHz) and provided scenes with on-ground resolution 3 km and swath width ~1,000 km.  
 159 The active sensor (radar) was only in operation until July 2015, whereas the passive radiometer is still  
 160 operating. We used the SPL4SMGP product (Reichle et al., 2015) with spatial resolution of 9 km for  
 161 root zone soil moisture estimation (0–100 cm; wetness units,  $\text{m}^3 \text{m}^{-3}$ ). This product utilizes SMAP's  
 162 microwave brightness temperature at 36 km and GEOS-5 Forward Processing Model Data from the  
 163 NASA Global Modeling and Assimilation Office at NASA's Goddard Space Flight Center. Data were  
 164 downloaded from (<https://n5eil01u.ecs.nsidc.org/SMAP>).

### 165 2.7.2. MERRA-2 data

166 MERRA-2 used observation-based precipitation data as forcing for the land surface  
 167 parameterization (Global Modeling..., 2015). Data (with spatial resolution  $0.5^\circ \times 0.625^\circ$ ) are available  
 168 since 1980. MERRA-2 monthly data were used for water content estimates within the "root zone" (0–  
 169 100 cm). We used the MERRA2 M2TMNXLND product  
 170 (<http://disc.sci.gsfc.nasa.gov/uui/search/%22MERRA-2%22>).

### 171 2.7.3. SPEI drought index analysis

172 We analyzed relationship between Siberian pine and fir mortality and SPEI values. For this  
 173 purpose, a map of major droughts (SPEI three major minimums,  $SPEI_{\min}$ ) was generated based on  
 174 following equation:

$$175 \quad SPEI_{\min,x,y} = \min_1(SPEI_{x,y}) + \min_2(SPEI_{x,y}) + \min_3(SPEI_{x,y}), \quad (1)$$

176 where  $\min_1, \min_2, \min_3$  are SPEI minimums within the  $i, j$  grid cells;  $x, y$  – are cells coordinates.  
 177 Then, within each grid cell regression analysis was performed (i.e.,  $SPEI_{\min}$  vs number of test sites  
 178 with tree mortality). The range of  $SPEI_{\min}$  values was divided into five classes (with ranges: -2 to -4; -4  
 179 to -6; -6 to -8; -8 to -10; -10 to -12). Then, for each of these classes the  $SPEI_{\min}$  and number of test  
 180 sites ( $N_{ts,i}$ ) was determined. After that  $N_{ts,i}$  was normalized by the following procedure:

181

$$182 \quad N_{norm,ts,i} = N_{ts,i} / N_{SPEI_{min},i} \quad (2)$$

183

184 where  $N_{norm,ts,i}$  – the normalized number of on-ground TS with tree mortality;  $N_{SPEI_{min},i}$  – a number  
 185 of pixels in  $i$ -th class of  $SPEI_{min}$ . Finally, regressions between  $N_{norm,ts,i}$  and  $SPEI_{min}$  were conducted.

#### 186 2.7.4. GRACE data

187 GRACE gravimetric data (available since 2003) were applied for detection of soil water  
 188 anomalies. We used monthly EWTA (Equivalent of Water Thickness Anomalies). EWTA accuracy is  
 189 10–30 mm month<sup>-1</sup> with spatial resolution 1° × 1° (Landerer and Swenson, 2012; Long et al., 2014;  
 190 <http://www.grace.jpl.nasa.gov>). Using analysis similar to SPEI above the relationship between  
 191 Siberian pine and fir mortality and EWTA values was analyzed. Similarly,  $EWTA_{min}$  was generated  
 192 based on equation (3):

$$194 \quad EWTA_{min,x,y} = \min_1(EWTA_{x,y}) + \min_2(EWTA_{x,y}) + \min_3(EWTA_{x,y}), \quad (3)$$

195  
 196 where  $\min_1$ ,  $\min_2$ ,  $\min_3$  – are three major EWTA May-Jul minimums of EWTA for each  $(x, y)$  grid  
 197 cell. TS normalization was similar to equation (2):

$$199 \quad N_{norm,ts,i} = N_{ts,i} / N_{EWTA_{min},i} \quad (4)$$

200  
 201 where – the normalized number of TS;  $N_{SPEI_{min},i}$  – a number of pixels in  $i$ -th class of  $EWTA_{min}$ .

#### 202 2.8. Dendrochronology analysis

203 Dendrochronology dataset included 180 *Pinus sibirica* and 50 *Abies sibirica* cores and disks  
 204 taken at breast height (1.3 m) by increment borer Tree ring width (TRW) was measured with 0.01 mm  
 205 precision using a linear table instrument (LINTAB-III). The TSAP and COFECHA computer  
 206 programs were used in tree ring analysis and cross dating of chronology (Rinn, 2003). Dates of tree  
 207 mortality were determined based on the master-chronology method (Fritts, 1991). For *Pinus sibirica*

208 an initial master chronology was constructed based on 28 living trees from a control site (no signs of  
 209 damage). The dataset was divided into “survivors” ( $N = 69$ ) and “decliners” ( $N = 83$ ) groups based on  
 210 radial increment trends during 2000–2014. Trees with a positive tree ring increment trend formed a  
 211 “survivors” cohort, whereas trees with a negative increment trend and dead trees formed “decliners”  
 212 cohort. “Control” group included the above mentioned 28 trees. For both cohorts standard  
 213 chronologies were constructed. Standard chronologies were indexed using ARSTAN software (i.e.,  
 214 detrending to remove long-term trends by negative exponential curve and a linear regression of  
 215 negative slope or horizontal line; Cook and Holmes, 1986). The resulting chronologies were a unitless  
 216 index of radial tree growth. For *Abies sibirica* chronologies were constructed for each ( $N = 3$ ) site. In  
 217 addition, chronologies with negative trends ( $N = 2$ ) were combined. The dataset was then divided into  
 218 “growth-release sites” ( $N = 16$ ) and “growth-depressed sites” ( $N = 34$ ).

### 219 3. Results

#### 220 3.1. DNC growth: dendrochronology data

221 Tree ring width (TRW) analysis showed that Siberian pine increment decreased since the  
 222 middle of the 1980s. That decrease coincided with increases in VPD and drought, and root zone  
 223 wetness decrease (Figs 2, 3). After a severe drought in 2003 trees were divided into “dead and  
 224 decliners” and “survivors” cohorts (Fig. 2). Trees also decreased growth at the control site, although  
 225 there were no visible signs of decline.

226 Fir trees response to ecological variables was more complicated. Within the “growth-depressed”  
 227 site TRW decreased, whereas at the “growth-released” site TRW increased after the 2003 drought  
 228 (Appendix Fig. A2). The latter site was composed of Siberian pine (upper canopy) and fir (lower  
 229 canopy). After the 2003 drought nearly 100% Siberian pine trees were died.

#### 230 3.2. DNC growth: relationship with climatic variables

231 The Siberian pine “decliners” cohort showed strong sensitivity to climate variables (Fig. 3). That  
 232 is, TRW had the highest correlation with SPEI ( $r = 0.89$ ;  $p < 0.001$ ). It is worth noting the significant  
 233 correlation with prior year precipitation ( $r = 0.46$ ;  $p < 0.01$ ). For the “survivors” cohort a significant  
 234 correlation was found only with VPD ( $r = 0.58$ ;  $p < 0.01$ ).

235 Similar to Siberian pine, fir trees from “growth depressed” site (“decliners”) were sensitive to  
 236 climate variables (the highest correlation was with SPEI,  $r = 0.74$ ,  $p < 0.001$ ; Appendix Fig. A3).

237 TRW was also significantly correlated with prior year precipitation ( $r = 0.48, p < 0.005$ ).

### 238 3.3. *DNC growth: dependence on soil moisture*

239 The SMAP model derived root zone moisture map of Lake Baikal Region showed that within the  
240 Khamar-Daban Ridge, the greatest stand mortality was observed at locations where the lowest soil  
241 water content was observed (Fig. 4).

242 Growth of the “decliners” Siberian pine cohort was found to be correlated with current year  
243 (July) root zone wetness ( $r = 0.62\text{--}0.85, p < 0.05$ ; Fig. 5). A higher correlation was observed for  
244 growth and prior year (July) root zone wetness ( $r = 0.76, p < 0.05$ ; Fig. 5). Fir showed similar  
245 sensitivity to the root zone wetness with correlations of  $r = 0.62$  ( $p < 0.001$ ) and  $r = 0.67$  ( $p < 0.001$ )  
246 for current and prior year measurements, respectively (Appendix Fig. A4).

### 247 3.4. *DNC mortality: relationship with relief features*

248 The spatial patterns of dead stands and “all stands” (i.e., before mortality) were significantly  
249 different. Dead stands were found on steeper south-west convex slopes and at higher elevations (Fig.  
250 6). The slope median of dead stands was  $17^\circ$ , whereas the median of all stands was at  $12^\circ$  (Fig. 6b).

251 It is interesting to note a predisposing “exposure effect” at the scale of individual trees. Since  
252 tree decline often begins on the sunlit side of the bole (Appendix Fig. A5) bark beetles primarily attack  
253 the “stressed” bole surface, whereas the bole’s northern side was still resistant to insect attacks  
254 (Appendix Figs A5b, A5c).

### 255 3.5. *Biotic impact*

256 We observed that within all test sites (with the exception of the control) Siberian pine and fir  
257 trees exhibited signs of bark and wood borer beetles attacks (i.e., *Pityogenes conjunctus* Rtt.,  
258 *Monochamus urussovi* Fischer.). Along with that, survey data (Review of forest heath..., 2010) also  
259 indicated some bacterial diseases and root fungi attacks.

### 260 3.6. *Area estimation of dead and declining DNC stands*

261 Within the major dieback area (rectangle on Fig. 1) dead stands occupied about  $\sim 5.4\%$  of the  
262 total DNC area. Severely damaged (i.e., stands with 50–75 % of dead trees) occupied  $\sim 4.2\%$  of the

263 DNC area. Thus, the total fraction of dead and declining stands was about 10 %. Within the whole  
 264 Khamar-Daban Ridge area about 9 % of DNC stands were severely damaged or dead.

### 265 3.7. *Tree mortality within the DNC range*

266 Siberian pine and fir mortality was documented within the vast southern part of these species range in  
 267 Siberia (Figs 7a, 8a). Significant correlations were found between DNC mortality and drought index  
 268 and soil water anomalies ( $r = -0.75, p < 0.1$  and  $r = 0.99, p < 0.01$ , respectively; Figs 7b, 8b).

## 269 4. Discussion

270 Within the Lake Baikal watershed Siberian pine and fir growth was observed to decrease since the  
 271 1980s. This decrease coincided with increased aridity (i.e., observed long-term decrease in drought  
 272 index). Water stress and severe drought split trees into “survivors” and “decliners” cohorts with an  
 273 obvious “turning point” in the 2000s after severe drought (see Fig. 2). Root zone wetness, the major  
 274 determinant of tree vigor, was also observed to decrease since the 1980s.

275 Spatial patterns of “survivors” and “decliners” were significantly different with decliners  
 276 located mainly on south facing convex steep slopes. Survivors occurred on relief features with less  
 277 water-stress (i.e., north facing concave slopes with less slope steepness).

278 Along the elevation gradient maximum tree mortality was observed within the elevation range  
 279 of 1,000–1,500 m. At lower elevations along the shoreline, water stress was reduced by Lake Baikal's  
 280 impact, whereas at higher elevations precipitation and relative humidity were increasing along the  
 281 elevation gradient. Tree ring width of “decliners” was correlated with vapor pressure deficit, drought  
 282 index SPEI, and root zone wetness. It is worth noting that TRW was also correlated with prior year  
 283 precipitation and root wetness zone (Fig. 5). A similar effect has been reported in other studies. For  
 284 example, Colenutt and Luckman (1991) showed that *Picea engelmannii*, *Abies lasiocarpa*, and *Larix*  
 285 *lyallii* are strongly influenced by prior year precipitation and growing conditions. Soil water anomalies  
 286 of the previous year also had a pronounced effect on *Larix gmelinii* growth and spruce *Picea abies*  
 287 decline in Belarus (Kharuk et al., 2015a,b). In the case of Lake Baikal forests, significant correlations  
 288 with prior year conditions indicate that trees are predisposed to biotic attacks. Signs of bark beetle and  
 289 wood borer attacks were observed within all the test sites with the exception of the control. Similarly,  
 290 extensive beetle outbreaks across the Engelmann spruce range in the United States were considered as  
 291 a consequence of a trend of warmer and drier climatic conditions (O'Connor et al., 2015; Kolb et al.,  
 292 2016). Synergy of drought and biotic impact was also reported for *Abies sibirica* stands in Southern

293 Siberian Mountains (Kharuk et al., 2016). On the other hand, intense drought itself may increase bark  
294 beetle activity and, consequently, increase tree mortality (Kolb et al., 2016).

295 Our results show Siberian pine experienced significant climate-induced growth decrease, which  
296 is attributed to the high precipitation sensitivity of this species (i.e., known in Russia as “the tree-of-  
297 fogs”). Observed fir growth decrease was less because fir forms the lower canopy and was partly  
298 protected from water stress by the shading effect of the upper canopy of Siberian pine. In addition,  
299 Siberian pine mortality facilitated fir growth release (Appendix Fig. A2) due to decreased competition  
300 for light and nutrients. Similarly, canopy protection facilitated regeneration survival of both species.  
301 Overgrowth of trees also caused stand mortality in some cases (e.g., Man’ko et al., 1998), but that is  
302 not the case for Baikal forests, where the mean age of Siberian pine and fir were 90 and 105 yrs.,  
303 respectively. One of the reasons for high drought-sensitivity of Siberian pine and fir is high leaf area  
304 index (LAI), a major determinant of water balance. Mixed DNC stands had LAI up to 7–8, whereas  
305 LAI of drought tolerant *Pinus silvestris* stands are about 3–4 (Utkin, 1975, re-calculated data).  
306 Therefore, a high LAI of Siberian pine and fir leads to intolerance to low humidity. This agrees with  
307 our observed high correlations between TRW and VPD and SPEI (Figs 3, Appendix A3).

308 The geographical location of Lake Baikal forests are within the margins of the ranges of  
309 Siberian pine and fir and determines the high sensitivity to climate variables anomalies. Eastward and  
310 southward, these precipitation-sensitive stands have given way to more drought-resistant larch and  
311 Scots pine stands. Similarly, across the whole of Siberia DNC decline and mortality was observed  
312 within the southern portion of these species area (Figs 7, 8). Siberian pine and fir mortality was  
313 strongly correlated with soil moisture anomalies and SPEI drought index within the range of these  
314 species.

## 315 5. Conclusion

316 Lake Baikal is strongly dependent on the health of its watershed. Composed of Siberian pine  
317 and fir, the forests in these watersheds have experienced growth decrease and mortality since the 1980s  
318 that coincides with increased aridity and a decrease of root zone wetness. Dead stands were located  
319 mainly within relief features with highest water stress risk. Tree decline started from lower relief  
320 features, decreasing along with elevation because of the increased humidity and precipitation. Water  
321 stress predisposed trees to attacks by pathogens. The synergy of these impacts caused Siberian pine  
322 and fir mortality on about 10% of “dark needle conifer” of the Lake Baikal watershed stands.

323 Biogeographically Lake Baikal forests are located within the boundary between the “dark  
324 needle conifer” range and the southward forest-steppe ecotone populated with drought-resistant Scot

325 pine and larch. Similar phenomena are observed for the whole range of DNC species in Siberia, where  
 326 mortality has occurred primarily within ecotones of “DNC and drought-resistant species”. Within the  
 327 interior of DNC range mortality is located with relief features with maximum water stress risk (i.e.,  
 328 steep convex southward slopes with shallow well-drained soils).

329 DNC mortality in Siberia is strongly correlated with SPEI drought index and soil moisture  
 330 anomalies ( $r = -0.75$ ,  $p < 0.1$  and  $r = 0.99$ ,  $p < 0.01$ , respectively). Predicted aridity increase in  
 331 southern Siberia (Climate Change, 2014), along with water-stress impact on trees, will also stimulate  
 332 pest outbreaks. The synergy of water stress and insects attacks will lead to elimination of the  
 333 precipitation sensitive “dark needle conifer” across the southern part of DNC range and its substitution  
 334 by drought-resistant species (e.g., *Pinus silvestris*, *Larix sibirica*, *L. gmelinii*). DNC, in turn, are  
 335 migrating now into northern larch-dominant communities (Kharuk et al., 2004).

336 The observed DNC decline within these species current range raises a question about  
 337 reforestation within dead stands. In the light of observing and expected climate change, precipitation-  
 338 sensitive Siberian pine and fir are not good for reforestation within observed areas of stands decline  
 339 and mortality. This issue needs more study.

#### 340 **Acknowledgements**

341 This research was supported by Russian Science Fund (RNF) [grant No. 14-24-00112] and by  
 342 NASA’s Terrestrial Ecology Program. The Landsat data processing was supported by the Ministry of  
 343 Education and Science of the Russian Federation (No. 2.914.2014/K).

#### 344 **References**

- 345 Aitken, S.N., Yeaman, S., Holliday, J.A., Wang, T., Curtis-McLane, S., 2008. Adaptation, migration or  
 346 extirpation: Climate change outcomes for tree populations. *Evol. Appl.* 1(1), 95–111.
- 347 Allen, C.D., Macalady, A.K., Chenchouni, H., Bachelet, D., McDowell, N., Vennetier, M., Kitzberger,  
 348 T., Rigling, A., Breshears, D.D., Hogg, E.H., Gonzalez, P., Fensham, R., Zhang, Z., Castro, J.,  
 349 Demidova, N., Lim, J., Allard, G., Running, S.W., Semerci, A., Cobb, N., 2009. A global  
 350 overview of drought and heat-induced tree mortality reveals emerging climate change risks for  
 351 forests. *For. Ecol. Manage.* 259, 660–684.
- 352 Congalton, R., 1991. A Review of Assessing the Accuracy of Classifications of Remotely Sensed  
 353 Data. *Remote Sens. Environ.* 37, 35–46.
- 354 Chuprova, N.P., 2008. About problem of spruce decay in European North of Russia. *Russian Forestry* 1,  
 355 24–26 (in Russian).

- 356 Climate Change 2014: Impacts, Adaptation, and Vulnerability IPCC Working Group II Contribution to  
357 AR5, 2014. Yokohama, Japan.
- 358 Colenutt, M.E., Luckman, B.H., 1991. Dendrochronological investigation of *Larix lyallii* at Larch  
359 Valley, Alberta. *Can. J. For. Res.* 21(8), 1222–1233.
- 360 Cook, E.R., Holmes R.L., 1986. Chronology development, statistical analysis, Guide for computer  
361 program ARSTAN, pp. 50–65. Laboratory of Tree Ring Research, the University of Arizona.
- 362 Fettig, C.J. Reid, M.L., Bentz, B.J., Sevanto, S., Spittlehouse, D.L., Wang, T., 2013. Changing  
363 climates, changing forests: A western North American perspective. *Journal of Forestry* 111(3),  
364 214–228.
- 365 Fritts, H.C., 1991. Reconstruction Large-scale Climatic Patterns from Tree-Ring Data: A Diagnostic  
366 Analysis. University of Arizona Press, Tucson.
- 367 Global Modeling and Assimilation Office (GMAO), 2015. MERRA-2 tavgM\_2d\_lnd\_Nx: 2d,  
368 Monthly mean, Time-Averaged, Single-Level, Assimilation, Land Surface Diagnostics, version  
369 5.12.4, Greenbelt, MD, USA: Goddard Space Flight Center Distributed Active Archive Center  
370 (GSFC DAAC), < [http://disc.sci.gsfc.nasa.gov/uui/datasets/M2TMNXLND\\_V5.12.4/](http://disc.sci.gsfc.nasa.gov/uui/datasets/M2TMNXLND_V5.12.4/)  
371 [summary?keywords=%22MERRA-2%22#citation](http://disc.sci.gsfc.nasa.gov/uui/datasets/M2TMNXLND_V5.12.4/)> (accessed August 2016).
- 372 Kharuk, V.I., Im, S.T., Ranson, K.J., Naurzbaev M.M., 2004. Temporal dynamics of larch in the  
373 forest-tundra ecotone. *Doklady Earth Science* 398(7), 1020–1023.
- 374 Kharuk, V.I., Im, S.T., Oskorbin, P.A., Petrov, I.A., Ranson, K.J., 2013a. Siberian Pine Decline and  
375 Mortality in Southern Siberian Mountains. *For. Ecol. Manage.* 310, 312–320.
- 376 Kharuk, V.I., Ranson, K.J., Oskorbin, P.A., Im, S.T., Dvinskaya, M.L., 2013b. Climate induced birch  
377 mortality in trans-Baikal lake region, Siberia. *For. Ecol. Manage.* 289, 385–392.
- 378 Kharuk, V.I., Im, S.T., Dvinskaya, M.L., Golukov, A.S., Ranson, K.J., 2015a. Climate-induced  
379 mortality of spruce stands in Belarus. *Environmental Research Letters* 10, 125006.
- 380 Kharuk, V.I., Ranson, K.J., Im, S.T., Petrov, I.A., 2015b. Climate-induced larch growth response  
381 within Central Siberian permafrost zone. *Environ. Res. Lett.* 10, 125009.
- 382 Kharuk, V.I., Petrov, I.A., Im, S.T., Yagunov, M., 2016. Pre-Baikal “dark taiga” stand’s decline.  
383 *Contemp. Probl. Ecol.* (accepted).
- 384 Kolb, T.E., Fettig, C.J., Ayres, M.P., Bentz, B.J., Hicke, J.A., Mathiasen, R., Stewart, J.E., Weed, A.S.  
385 2016. Observed and anticipated impacts of drought on forests insects and diseases in the United  
386 States. *For. Ecol. Manage.*, early online, <http://dx.doi.org/10.1016/j.foreco.2016.04.051>.
- 387 Landerer, F.W., Swenson, S.C., 2012. Accuracy of scaled GRACE terrestrial water storage estimates.  
388 *Water Resour. Res.* 48, W04531.

- 389 Lloyd, A.H., Bunn, A.G., 2007. Responses of the circumpolar boreal forest to 20th century climate  
390 variability. *Environ. Res. Lett.* 2, 045013.
- 391 Logan, J.A., Regniere, J., Powell, J.A., 2003. Assessing the impacts of global warming on forest pest  
392 dynamics. *Front. Ecol. Environ.* 1, 130–137.
- 393 Long, D, Longuevergne, L., Scanlon, B.R., 2014. Uncertainty in evapotranspiration from land surface  
394 modeling, remote sensing, and GRACE satellites. *Water Resour. Res.* 50, 1131–1151.
- 395 Man'ko, Y.I., Gladkova, G.A., Butovets, G.N., Kamibayasi, N., 1998. Monitoring of fir-spruce forests  
396 decay in the Central Sikhote-Alin. *Russian Forest Sciences* 1, 3–16 (in Russian).
- 397 Martínez-Vilalta, J., Lloret, F., Breshears, D.D., 2012. Drought-induced forest decline: causes, scope  
398 and implications. *Biol. Lett.* 8, 689–691.
- 399 Millar, C.I., Stephenson, N.L., 2015. Temperate forest health in an era of emerging megadisturbance.  
400 *Science* 21, 823–826.
- 401 O'Connor, C.D., Lynch, A.M., Falk, D.A., Swetnam, T.W., 2015. Post-fire forest dynamics and  
402 climate variability affect spatial and temporal properties of spruce beetle outbreaks on a Sky  
403 Island mountain range. *For. Ecol. Manage.* 336, 148–162.
- 404 Pavlov, I.N., Ruhullaeva, O.V., Barabanova, O.A., Ageev, A.A., 2008. Estimation of root pathogens  
405 impact on forest resources of Siberian federal district. *Boreal Zone Conifers* 25, 262–268 (in  
406 Russian).
- 407 Raffa, K.F. Aukema, B.H., Bentz, B.J., Carroll, A.L., Hicke, J.A., Turner, M.G., Romme, W.H., 2008.  
408 Cross-scale drivers of natural disturbances prone to anthropogenic amplification: the dynamics  
409 of bark beetle eruptions. *Bioscience* 58, 501–517.
- 410 Reichle, R., De Lannoy, G., Koster, R.D., Crow, W.T, Kimball, J.S., 2015. SMAP L4 9 km EASE-  
411 Grid Surface and Root Zone Soil Moisture Geophysical Data, Version 1. Boulder, Colorado  
412 USA. NASA National Snow and Ice Data Center Distributed Active Archive Center.  
413 <http://dx.doi.org/10.5067/HJK4FUNIML52> (accessed February 2015).
- 414 Review of forest health in the Buryatia Republic, 2010. Ulan-Ude: Phil. Roslesozashchita, 102–105 (in  
415 Russian).
- 416 Riano, D., Chuvieco, E., Salas, J., Aguado, I., 2003. Assessment of different topographic corrections in  
417 Landsat-TM data for mapping vegetation types. *IEEE Trans. Geosci. Remote Sens.* 41(5). 1056–  
418 1061.
- 419 Rinn, F., 2003. TSAP-Win User Reference Manual. Rinntech, Heidelberg, <http://www.rinntech.com>.
- 420 Sarnatskii, V.V., 2012. Zonal-typological patterns of periodic large-scale spruce decay in Belarus.  
421 *Proc. of BGTU. Forest estate*, 274–276 (in Russian).

- 422 Utkin, A.I., 1975. Biological productivity of forests: study methods and results. *Forestry and*  
423 *silviculture* 1, 9–189 (in Russian).
- 424 Yousefpour, R., Hanewinkel, M., Le Moguédec, G., 2010. Evaluating the Suitability of Management  
425 Strategies of Pure Norway Spruce Forests in the Black Forest Area of Southwest Germany for  
426 Adaptation to or Mitigation of Climate Change. *Environ. Manage.* 45, 387.
- 427 Vicente-Serrano, S.M., Beguería, S., López-Moreno, J.I., 2010. A Multiscalar Drought Index Sensitive  
428 to Global Warming. The Standardized Precipitation Evapotranspiration Index. *J. Clim.* 23, 1696–  
429 1718.
- 430 Zamolodchikov, D.G., 2011. Evaluation of climate-induced changes in diversity of tree species  
431 according to forest fond data records. *Biology Bulletin Reviews* 131, 382–392 (in Russian).

432 **Figure legends**

433 **Fig. 1.** The study area location (Khamar-Daban Ridge). The right insert image expands this area and  
 434 shows the location of major DNC mortality (rectangle) and field test sites (white discs). DNC stands  
 435 are shown by dark tones on image. Left insert image is a photo of declining stands.

436 **Fig. 2.** Siberian pine tree ring chronologies vs SPEI, vapor pressure deficit (VPD), and root zone  
 437 wetness. Drought dates: 2003, 2006, 2010 and 2015. Note: SPEI drought index increase means drought  
 438 decrease, and vice versa. Trends are significant at  $p < 0.01$ .

439 **Fig. 3.** Relationship between Siberian pine TRW (“decliners” cohort;  $N = 83$ ) and (a) air temperature  
 440 (current year June), (b) precipitation (prior year July), (c) vapor pressure deficit (current year June),  
 441 and (d) SPEI (current year May-August). Analyzed period: 1985–2013. Note: SPEI decrease means  
 442 drought increase, and vice versa.

443 **Fig. 4.** SMAP-derived map of root zone wetness within Baikal Lake area (July 2015). Legend units  
 444 are  $m^3 m^{-3}$ . Rectangle denotes an area of major Siberian and pine and fir mortality. Black dots  
 445 indicate the locations of dead stands.

446 **Fig. 5.** Relationship between Siberian pine TRW and soil wetness. (a, b) – TRW (“decliners” cohort)  
 447 vs root zone wetness in July of prior (a) and current (b) year. Analyzed period: 1985–2013. (c) – TRW  
 448 (“decliners”) vs soil water anomalies (EWTA in current year minimum). Analyzed period: 2003–2009.  
 449 (d) – TRW (“survivors”) vs soil water anomalies (1 – prior and 2 – current year, respectively).  
 450 Analyzed period: 2003–2014.

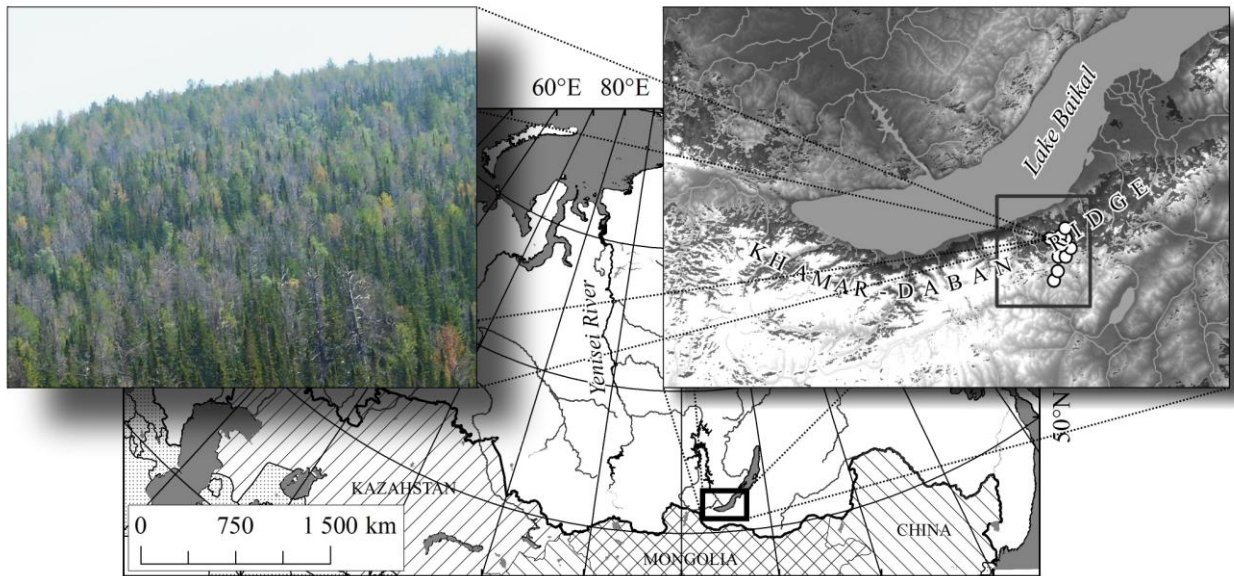
451 **Fig. 6.** Spatial distributions of (1) “dead and declining” and (2) all stands (within rectangle on Fig. 1).  
 452 (a-d): “dead and declining” stands vs (a) elevation, (b) slope steepness (medians shown as vertical  
 453 dashed lines), (c) exposure, and (d) surface curvature (concave is negative, convex is positive).

454 **Fig. 7.** (a) Map of SPEI minimums ( $SPEI_{min}$  for May-Aug, 2002–2015; 1, 2 – Siberian pine and fir  
 455 ranges, respectively). Test sites with stand mortality are denoted as white disks. (b) The percentage of  
 456 test sites with stand mortality ( $N = 9681$  vs the drought index  $SPEI_{min}$ ).

457 **Fig. 8.** (a) Map of soil water anomalies minimums ( $EWTA_{min}$  for May-July, 2002–2015; 1, 2 –  
 458 Siberian pine and fir ranges, respectively). Test sites with stand mortality are denoted as white disks.  
 459 (b) The percentage of test sites with stand mortality ( $N = 9681$ ) vs  $EWTA_{min}$ .

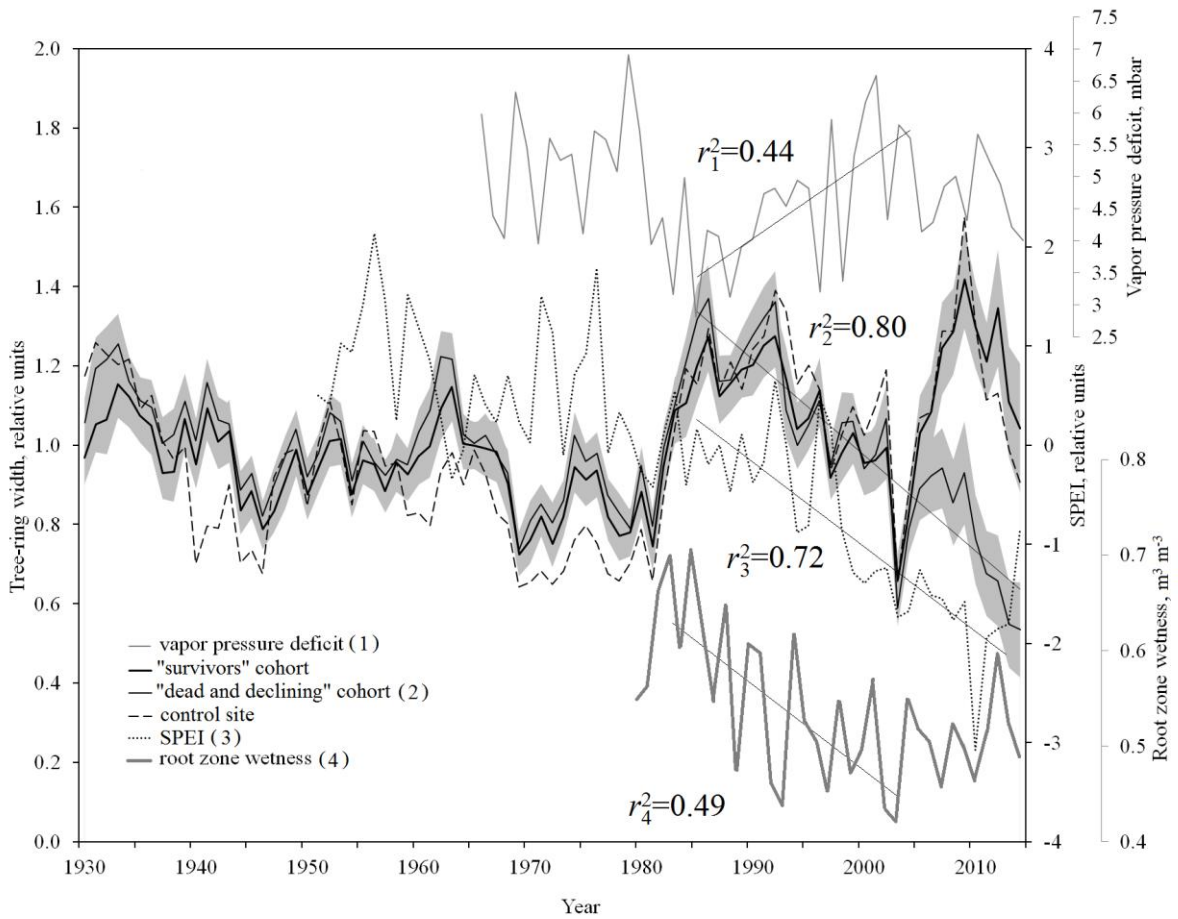
460

461 **Figure 1**



462

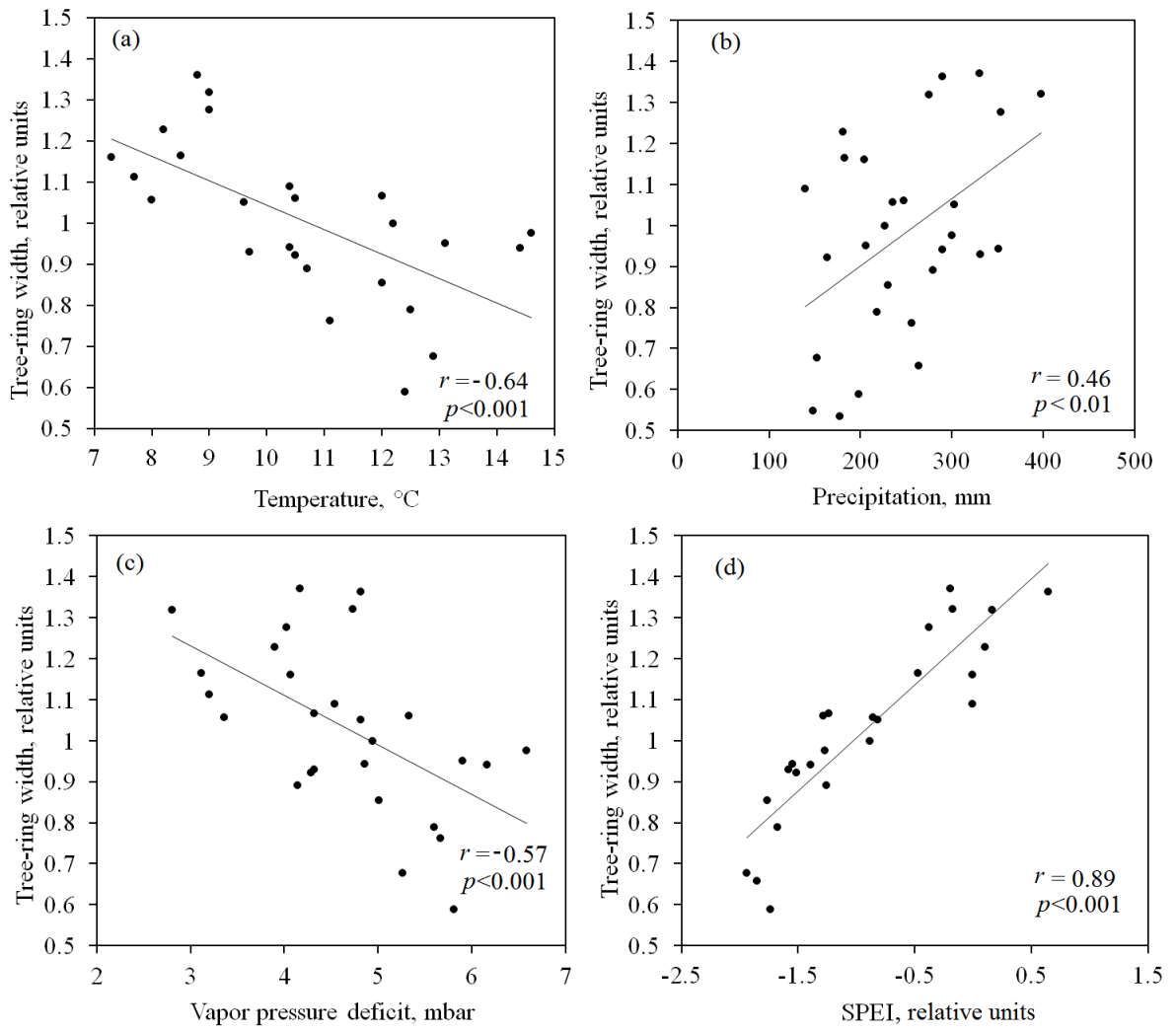
463 **Figure 2**



464

465

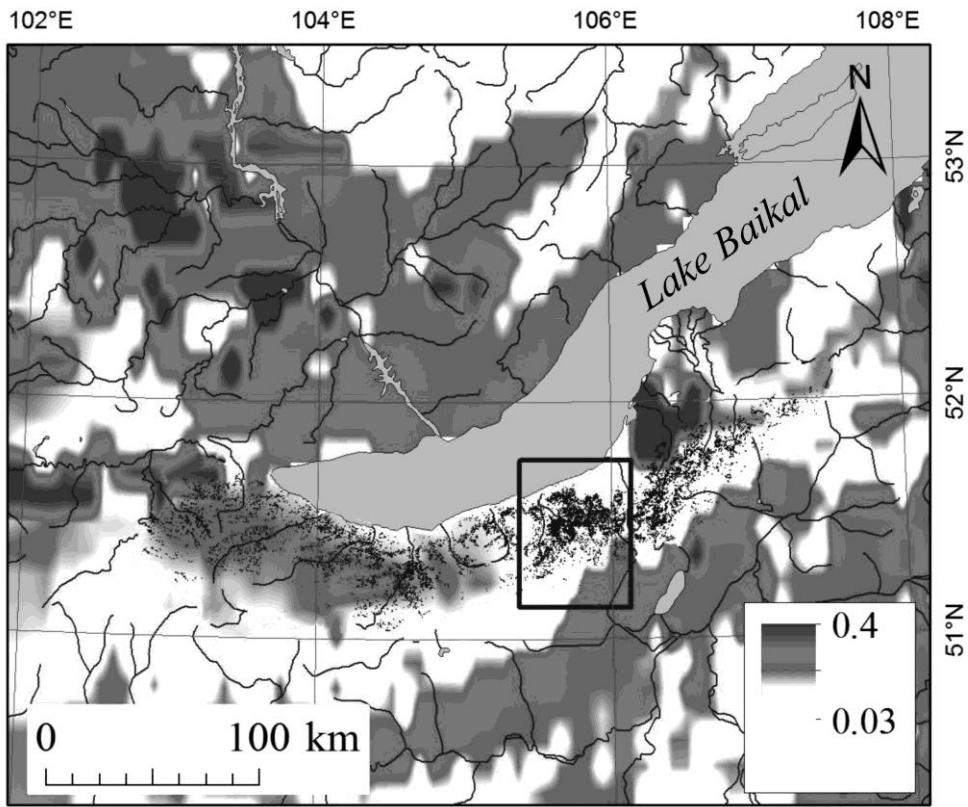
466 **Figure 3**



467

468

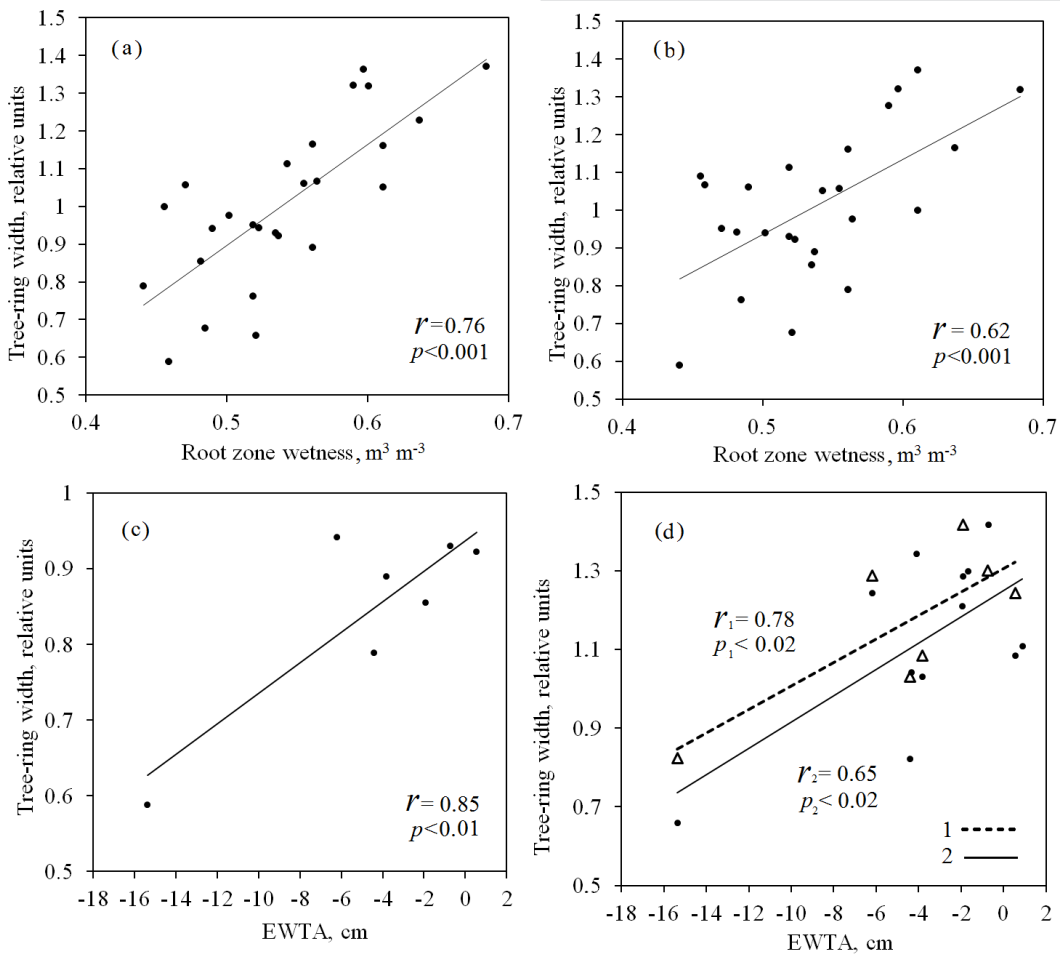
469 **Figure 4**



470

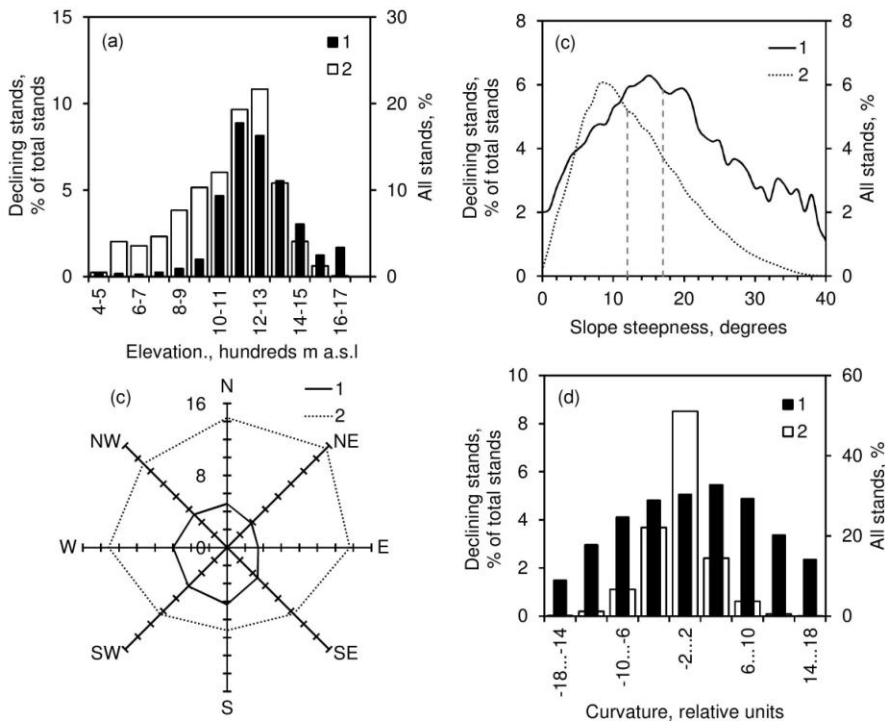
471

472 **Figure 5**



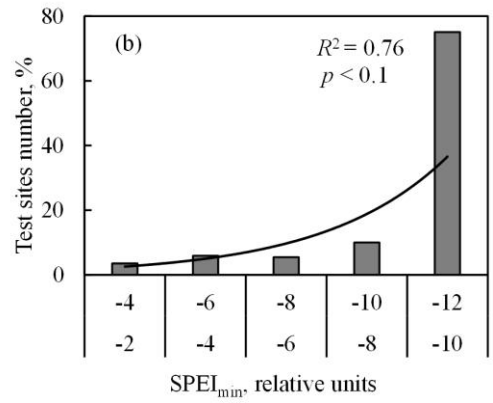
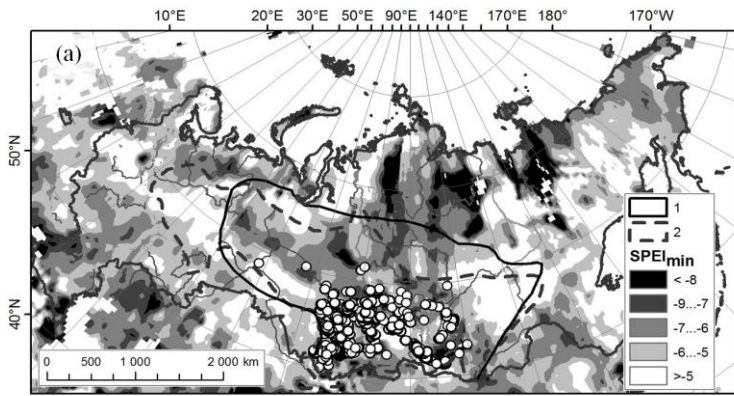
473

474 **Figure 6**



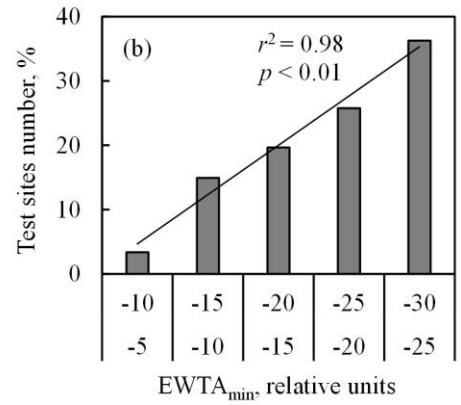
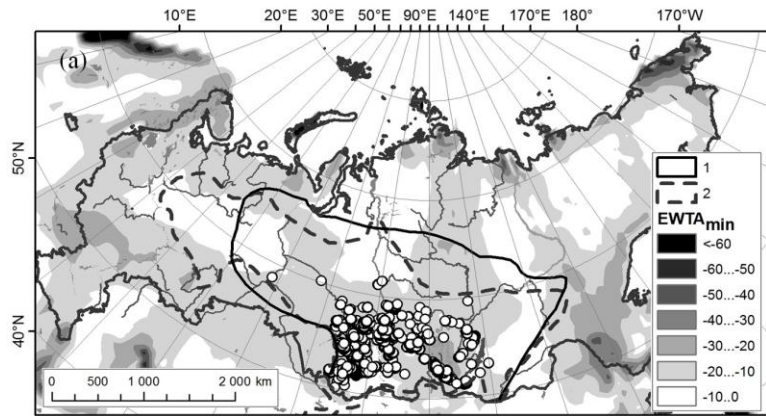
475

476 **Figure 7**



477

478 **Figure 8**



479

480